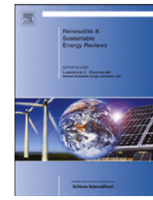
Renewable and Sustainable Energy Reviews 20 (2013) 155–168

Contents lists available at SciVerse ScienceDirect

Renewable and Sustainable Energy Reviews

journal homepage: www.elsevier.com/locate/rser



Experimental assessment of the solar energy potential in the gulf of Tunis, Tunisia

Ahmed Ridha El Ouderni, Taher Maatallah, Souheil El Alimi *, Sassi Ben Nassrallah

Energy and Thermal Systems Laboratory, National Engineering School of Monastir, University of Monastir, Avenue Ibn, El Jazzar 5019, Tunisia

ARTICLE INFO

Article history:
Received 15 November 2011
Received in revised form
3 November 2012
Accepted 5 November 2012
Available online 31 December 2012

Keywords:
Gulf of Tunis
Global solar Radiation
Model comparison
Solar energy potential

ABSTRACT

This work carries out the availability of the global solar radiation over the site of Borj-Cedria in the gulf of Tunis (36°43′04″N latitude and 10°25′41″E longitude), Tunisia. Global solar radiation variability was assessed on hourly, daily, monthly and seasonal scales. Solar potential in the gulf of Tunis was evaluated using the solar radiation data collected by the meteorological NRG weather station installed in the Center of Research and Technologies of Energy (CRTEn) in the Borj-Cedria area. The collected measurements during the last three years (2008, 2009 and 2010) were based on 10 min time step. These data have allowed us to evaluate the global solar flux, the sun duration, the yearly and the seasonal frequency distribution of the global solar radiation. Moreover, a conventional model has been used to estimate the hourly solar radiation on a horizontal plane and it has been validated by experimental measurements in specific days. The results show that the global solar radiation predicted by the conventional model has a good agreement with the experimental data during the clear sky conditions with a mean absolute percentage error (MAPE) of 4.1%. However, the limitation of the conventional model appears under the cloudy sky weather which is proved by the highest value of relative error percentage reaching 14.26% occurred during the autumnal equinox day.

Contents

* Corresponding author. Tel.: +216 98452098; fax: +216 73501597.
E-mail address: souheil.elalimi@gmail.com (S. El Alimi).

1364-0321/$ - see front matter © 2012 Elsevier Ltd. All rights reserved.
http://dx.doi.org/10.1016/j.rser.2012.11.016

1. Introduction

No doubt that all kind of energies took origin from the sun. This huge furnace, with a diameter of 1.39×10^9 m, emits a total energy output of 3.8×10^{20} MW, however only a tiny fraction of 1.7×10^{14} kW is intercepted by the earth. So that since the prehistoric times, man has realized that a good use of solar energy is in his benefit. Therefore, solar energy has been harnessed by mankind [1]. Indeed, the Greek physician Archimedes (212 BC) burned the Roman fleet by means of concave metallic mirror in the form of hundreds of polished shields; all reflecting on the same ship [1,2]. Then, Kircher (1601–1680) worked out some experiments to validate the story of Archimedes. Yet, no report of his findings survived [3].

Despite of the serious difficulties to apply the solar energy concentration, the use of concentrating collectors was the first application developed in this field. The construction of the first solar furnaces, capable of melting iron, copper and other metals, was recorded from the French scientist Lavoisier during the 18th century [1].

The furnaces were in use throughout Europe and the Middle East and attained the remarkable temperature of 1750 °C. The 19th century was marked by two important events; the first one was the discovery of the photovoltaic effect by Becquerel as a new form of solar energy exploitation. The second was related to the several attempts to convert solar energy into other forms based upon the generation of low pressure steam to operate steam engines. In fact, Monchot has built several solar-powered steam engines between the years 1864 and 1878 [3].

As the lack of water was always a problem to humanity, researchers attempted to harness solar energy by developing new equipment suitable for the desalination of sea-water. Consequently, solar distillation has been in practice for a long time. At the same period, the first water distillation plant was built at Las Salinas, Chile in 1874 [3,4], using solar stills that evaporate salty water. Besides, in Algeria Mouchot designed and set a truncated cone reflector in1875. Another furnace was set up in Algeria.

After that, Eneas installed a focusing collector to operate a water pumping apparatus at California farm in 1901 by concentrating the sun's rays at a focal point where the boiler was located. In 1904, a Portuguese priest, constructed a large solar furnace which appeared quite modern in structure, being a large, off-axis, parabolic horn collector [3].

In 1913, the world's largest pumping plant was implemented in Meadi, Egypt by Shuman, in collaboration with Boys using long parabolic cylinders to focal point sunlight into a long absorbing tube. In 1928, Pasteur has reported a novel way to use solar concentrators in solar distillation by focusing solar rays into a copper boiler containing water. The steam generated from the boiler was piped to a conventional water cooled condenser in which distilled water was accumulated [4].

Otherwise, the house heating and hot water appeared in the mid 1930s and recognized a real expansion in the last half of the 40s all over the world. The main solar water heaters were manufactured in many countries, for instance, the thermosyphon types which consist to a two flat-plate solar collectors having an absorber and storage tank.

On the other hand, the first practical application of solar cells was in space in the 1960s when scientists discovered other photovoltaic materials such as gallium arsenide (GaAS) which increased the cost of PV installation.

The global installed capacity of photovoltaics at the end of 2002 was near 2 GWp [5] Photovoltaic (PV) cells are made of various semiconductors, basically the silicon (Si), compounds of cadmium sulfide (Cds), cuprous sulfide (Cu2S), and GaAs which are materials that are only moderately good conductors of electricity. Thirty years ago, PV modules began to be for large-scale commercial applications with an efficiency below 10%. Nowadays, their efficiency is about 20% and estimated to reach 25% in 2020.

2. Recent studies

Knowledge of the availability of the global solar flux at the earth's surface has a great importance in solving many scientific problems and harnessing the practical utilization of solar energy. This available quantity of energy changes within geographic place because it depends on climatic and atmospheric conditions.

It is known that global solar radiation is poorly sampled in weather station networks. For this reason, we find in the literature, recently, many authors who attempted to develop several models to estimate the global solar radiation and asses their corresponding solar potential [6–23]. We can find also software packages allowing the solar flux density estimation of several sites.

Coskum et al. [24] have modified the concept of the probability density frequency usually used to analyze the wind and the outdoor temperature distributions in order to estimate the solar radiation distribution and therefore to investigate and design better the solar energy systems. They have also conducted their study with global solar irradiation data of many years recorded by the Turkish State Meteorological Service.

Ryder et al. [25] have used the solar irradiance measurements from a new high density urban network in London. They have measured annual averages and demonstrated that central London receives 30 ± 10 W m^{-2} less solar irradiance than outer London at midday, equivalent to 9 ± 3% less than the London average. They have obtained these measurements basing on a new technique referred to the 'Langley flux gradients' that infer aerosol column concentrations over a clear periods of 3 h and this technique has been developed and applied to three case studies.

The survey of Ramachandra et al. [26] has focused on the assessment of the Indian potential resource with variability derived from high resolution satellite data. They have also presented a techno-economic analysis of the solar power technologies and a prospective for a minimal utilization of the available land.

Sorapipatana [27] has adopted a satellite technique to assess solar energy potential in Kampuchea. In his work, he has estimated

the solar irradiation potential at an interval of half a degree grid. The seasonal variations of mean daily solar irradiation in Kampuchea were measured during two Asian winter and summer monsoon seasons.

Molero et al. [28] have developed a transient 3-D mathematical model for solar flat plate collectors. Their model is based on setting mass and energy balances on finite volumes and allows the comparison of different configurations. This model is a useful tool to improve the design of plate solar collectors and to compare different configurations.

Hocaoglu [29] proposed a solar radiation modeling approach using the hidden Markov models. This approach mean of hourly measured ambient temperature values are considered as observations of the model, whereas mean of hourly solar radiation values are considered as the hidden events, which constitute the outcomes of the proposed mathematical model. The proposed model exploited the inherent cross dependency between daily ambient temperature and solar radiation in a form of hidden Markov model (HMM) using the optimization technique called the Viterbi decoding algorithm.

Ozgoren et al. [30] developed an artificial neural network (ANN) model based on multi-nonlinear regression (MNLR) method for forecasting the monthly mean daily sum global solar radiation at any place of Turkey. This aim was based on the meteorological data of 31 stations spread over Turkey along the years 2000–2006. The developed model was very useful to calculate quickly and satisfactorily the monthly global solar radiation at any place of Turkey.

Maghrabi [31] established a simple model to estimate the monthly mean global solar radiation on a horizontal surface in Tabouk (Saudi Arabia) using 9 years of solar radiation data. The model correlated the global solar radiation with five meteorological parameters. These parameters were the perceptible water vapor, air temperature, relative humidity, atmospheric pressure, and the mean monthly daily fraction of possible sunshine hours. The obtained model showed its high accuracy for the monthly global solar radiation estimation in Tabouk and other places having similar conditions.

Mao and Li [32] evaluated the monthly mean daily solar radiation in Chongqing basing on the observed meteorological variables including daily maximum and minimum temperatures, daily mean dew point temperature, fog and rainfall analyzed from 1986 to 2000. Moreover, a newly developed model that included all selected variables proved the best method with a root mean squared error (RMSE). In fact, 12 models were developed however they performed differently in different seasons.

Moradi [33] developed a new and automatic method for controlling the quality of daily global solar radiation using sunshine duration hours. In fact, the proposed method was based on a three levels of tests: which were firstly the daily global solar radiation has to be compared against the daily extraterrestrial radiation that is received on a horizontal surface second, secondly the daily global solar radiation should only exceed by a small amount of the daily clear sky irradiation that was observed under highly transparent clear skies and thirdly the method used a series of persistence checks that utilized the relation between daily global solar radiation and relative sunshine duration hours. The method proved its ability e to identify the systematic and non-systematic errors under three different climates including semi-arid, coastal humid and very arid climates.

Voyant et al. [34] presented an application of Artificial Neural Networks (ANN) to predict the daily solar radiation. The authors proposed a contribution study of exogenous meteorological data compared with different forecasting methods. This study showed that the use of exogenous data generates a RMSE between 0.5% and 1% for two stations during 2006 and 2007 (Corsica Island, France). Besides, the prediction results were also relevant for the concrete case of a tilted PV wall. In fact, the addition of endogenous and exogenous data allowed a 1% decrease of the RMSE over 6 months-cloudy period for the power production. While the use of exogenous data showed an interest in winter, endogenous data as inputs on a preprocessed ANN appeared sufficient in summer.

Korachagaon and Bapat [35] developed a general formula to estimate the solar radiation with the local site parameters such as air temperature, relative humidity, wind, moisture and few derived parameters independent variables. The developed models were validated with remaining 665 data sites. Authors concluded that two candidate models should be proposed because they were are capable to cover 50% of the land area on earth surface between latitude ± 30 with an estimation error (RMSE) limiting to 15%. Thus, it was predicted that the proposed models can be used to estimate the monthly average daily global solar radiation in area where the radiation data is missing or not available.

Si-qing et al. [36] made a study on the medium-term forecast of solar 10.7 cm radio flux (F10.7). By comparing their forecast results in the period from 21th September 2005 to 7th June 2007, they have been demonstrated that the accuracy of the autoregressive forecast method is equivalent to that of the forecast made by the American Air Force.

In this study, an overview of research works of all over the global solar radiation models is presented. The mentioned models can be considered as the representative of worldwide average. Its details can be found therein. Moreover, we present a classic theoretical model of the solar flux density of sun in the site of the gulf of Tunis in Tunisia. This model is used to estimate the direct and the diffuse radiation.

We proceed to the validation of this model by experimental measurements which are conducted by means of a meteorological station during the period of 2008–2010 with a 10-min time step by the NRG weather station. The treatment of about 158,000 observations permit us to evaluate the global solar flux in the site of the gulf of Tunis.

3. Site description and experimental design

Tunisia is located in North Africa. It is bordered by Algeria to the west and Libya to the southeast. It is the northern most country on the African continent, and the smallest of the nations situated along the atlas mountain range (Fig. 1). The country is divided in two regions, the well-watered north and the semi-arid south. An abrupt southern turn of its shoreline gives Tunisia two faces on the Mediterranean Sea with 1298 km coastline. Fig. 1 shows also that Tunisia is situated in the most insolated regions of the globe for which the annual average global solar radiation exceed 2000 kWh/m^2/year. Fig. 2 shows the geographic localization of the Borj-cedria site in the gulf of Tunis.

The experimental design is a NRG station installed in 36°43′04″N latitude and 10°25′41″E longitude (Fig. 3). It provides the measurement of wind speed, wind direction, ambient temperature and the global solar flux in the gulf of Tunis [37]. This station is equipped with an acquisition system that record, every 10 min the average, the max, the min and the standard deviation values for each sensor.

4. Theoretical models of solar flux estimation: an overview

In the literature, several empirical models have been developed to estimate global solar radiation which depends on different



Fig. 1. Geographic position of Tunisia.

factors such as extraterrestrial radiation, sunshine hours, mean and maximum temperature, relative humidity, number of rainy days, altitude, latitude, the turbidity of the atmosphere and so forth [38–61]. In general, most of the widespread literature available on evaluating the surface solar flux can be categorized into two broad groups: monthly-averaged daily irradiation and monthly-averaged hourly irradiation.

4.1. Monthly-averaged daily radiation

Measured monthly-averaged values of daily irradiation H are an excellent basis of information and offer the starting point of many computation schemes. Angstrom (1924) proposed a correlation relating H and the monthly average of the instrument – recorded daily time fraction of bright sunshine S as follows [62]:

$$\frac{H}{H_0} = \alpha + (1-\alpha)S \tag{1}$$

where H_0 and α are the monthly average daily extraterrestrial radiation and location-based empirical constant ($\alpha = 0.25$ for Stockholm) respectively. Further efforts in the literature suggested additional empirical modifications to the Angstrom equation are illustrated in the following section.

4.1.1. Angstrom–Prescott–Page model

The Angstrom–Prescott–Page model is the most commonly used model as given by [63]:

$$\frac{H}{H_0} = a + b\frac{S}{S_0} \tag{2}$$

where H, H_0, S, S_0, a and b are the monthly average daily global radiation, the monthly average daily extraterrestrial radiation, the day length, the maximum possible sunshine duration, and two empirical coefficients respectively.

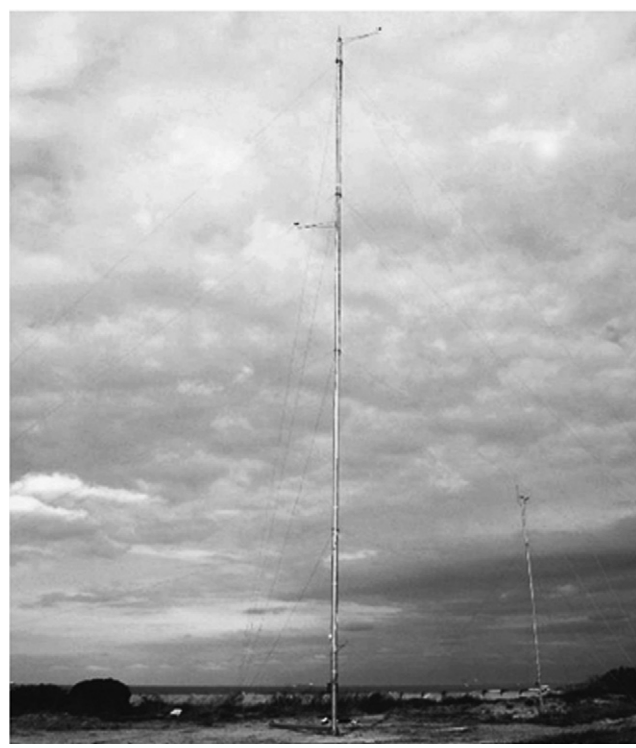


Fig. 2. Geographic localization of Borj Cedria site.

The monthly average daily extraterrestrial solar radiation on a horizontal surface can be given using the following equation [64,65]:

$$H_0 = \frac{24}{\pi} G_{on}\left[\cos\varphi \cos\delta \sin(w_s) + \frac{\pi}{180} w_s \sin\varphi \sin\delta\right] \tag{3}$$



Fig. 3. NRG weather station.

where G_{on} is normal extraterrestrial radiation, φ is the latitude of the site, δ is the solar declination and w_s is the mean sunrise hour angle for the given month. The normal extraterrestrial radiation, the solar declination and the sunrise hour angle can be computed by the following equations:

$$G_{on} = G_{sc}\left(1 + 0.033\cos\frac{360\,n}{365}\right) \tag{4}$$

where G_{sc} is solar constant which is defined as the energy from the sun per unit time received on a unit area of surface perpendicular to the direction of propagation of the radiation at mean earth–sun distance outside the atmosphere and n is the ordinal date. $n=1$ at January 1st and $n=365$ at December 31st.

$$\delta = 23.45^{\circ}\sin\left(360\frac{284+n}{365}\right) \tag{5}$$

$$w_s = \arccos(-\tan\varphi\tan\delta) \tag{6}$$

For a given month, the maximum possible sunshine duration S_0 can be estimated as follows [66]:

$$S_0 = \frac{2}{15}w_s \tag{7}$$

4.1.2. Tiris et al. model

Tiris et al. proposed the a and b empirical coefficients of the Angstrom–Prescott–Page model for Turkey, in general, as follows:

$$\frac{H}{H_0} = 0.18 + 0.62\frac{S}{S_0} \tag{8}$$

4.1.3. Page model

Page has given the coefficients of the Angstrom–Prescott–Page model, which is believed to be adopted all over the world, as the following [67]:

$$\frac{H}{H_0} = 0.23 + 0.48\frac{S}{S_0} \tag{9}$$

4.1.4. Bahel et al. model

Bahel et al. proposed the following relationship [68]:

$$\frac{H}{H_0} = 0.175 + 0.552\frac{S}{S_0} \tag{10}$$

4.1.5. Louche et al. model

Louche et al. suggested the following model to expect the global solar radiation [69]:

$$\frac{H}{H_0} = 0.206 + 0.546\frac{S}{S_0} \tag{11}$$

4.1.6. Benson et al. model

Benson et al. presented two different formulations for two periods of a year as the following [70]:

$$\frac{H}{H_0} = 0.18 + 0.60\frac{S}{S_0} \tag{12}$$

for the periods during January–March and October–December.

$$\frac{H}{H_0} = 0.24 + 0.53\frac{S}{S_0} \tag{13}$$

for the period between April and September.

4.1.7. Monthly specific Dogniaux and Lemoine model

Dogniaux and Lemoine proposed the following specific monthly correlations [71]:

$$\text{January}\ \frac{H}{H_0} = (-0.00301\delta + 0.34507) + (0.00495\delta + 0.34572)\frac{S}{S_0} \tag{14}$$

$$\text{February}\ \frac{H}{H_0} = (-0.00301\delta + 0.34507) + (0.00495\delta + 0.34572)\frac{S}{S_0} \tag{15}$$

$$\text{March}\ \frac{H}{H_0} = (-0.00303\delta + 0.36690) + (0.00466\delta + 0.36377)\frac{S}{S_0} \tag{16}$$

$$\text{April}\ \frac{H}{H_0} = (-0.00334\delta + 0.38557) + (0.00456\delta + 0.35802)\frac{S}{S_0} \tag{17}$$

$$\text{May}\ \frac{H}{H_0} = (-0.00245\delta + 0.35057) + (0.00485\delta + 0.33550)\frac{S}{S_0} \tag{18}$$

$$\text{June}\ \frac{H}{H_0} = (-0.00327\delta + 0.39890) + (0.00578\delta + 0.27292)\frac{S}{S_0} \tag{19}$$

$$\text{July}\ \frac{H}{H_0} = (-0.00369\delta + 0.41234) + (0.00568\delta + 0.27004)\frac{S}{S_0} \tag{20}$$

$$\text{August}\ \frac{H}{H_0} = (-0.00269\delta + 0.36244) + (0.00412\delta + 0.33162)\frac{S}{S_0} \tag{21}$$

$$\text{September}\ \frac{H}{H_0} = (-0.00338\delta + 0.39467) + (0.00564\delta + 0.27125)\frac{S}{S_0} \tag{22}$$

$$\text{October}\ \frac{H}{H_0} = (-0.00371\delta + 0.36213) + (0.00504\delta + 0.31790)\frac{S}{S_0} \tag{23}$$

$$\text{November}\ \frac{H}{H_0} = (-0.00350\delta + 0.36680) + (0.00523\delta + 0.31467)\frac{S}{S_0} \tag{24}$$

$$\text{December}\ \frac{H}{H_0} = (-0.00350\delta + 0.36262) + (0.00559\delta + 0.30675)\frac{S}{S_0} \tag{25}$$

4.1.8. Specific Monthly-Rietveld model

Soler used the Rietveld's model to 100 European stations and suggested the following specific monthly relationships [72]:

$$\text{January}\ \frac{H}{H_0} = 0.18 + 0.66\frac{S}{S_0} \tag{26}$$

$$\text{February}\ \frac{H}{H_0} = 0.20 + 0.60\frac{S}{S_0} \tag{27}$$

$$\text{March}\ \frac{H}{H_0} = 0.22 + 0.58\frac{S}{S_0} \tag{28}$$

$$\text{April}\ \frac{H}{H_0} = 0.20 + 0.62\frac{S}{S_0} \tag{29}$$

$$\text{May}\ \frac{H}{H_0} = 0.24 + 0.52\frac{S}{S_0} \tag{30}$$

$$\text{June}\ \frac{H}{H_0} = 0.24 + 0.53\frac{S}{S_0} \tag{31}$$

$$\text{July}\ \frac{H}{H_0} = 0.23 + 0.53\frac{S}{S_0} \tag{32}$$

$$\text{August}\ \frac{H}{H_0} = 0.22 + 0.55\frac{S}{S_0} \tag{33}$$

$$\text{September}\ \frac{H}{H_0} = 0.20 + 0.59\frac{S}{S_0} \tag{34}$$

$$\text{October}\ \frac{H}{H_0} = 0.19 + 0.60\frac{S}{S_0} \tag{35}$$

$$\text{November}\ \frac{H}{H_0} = 0.17 + 0.66\frac{S}{S_0} \tag{36}$$

$$\text{December}\ \frac{H}{H_0} = 0.18 + 0.65\frac{S}{S_0} \tag{37}$$

4.1.9. Gopinathan model

This model assumed to use the following Angstrom–Prescott–Page coefficients [73]:

$$a = 0.265 + 0.07Z - 0.135\left(\frac{S}{S_0}\right) \tag{38}$$

$$b = 0.401 + 0.108Z - 0.325\left(\frac{S}{S_0}\right) \tag{39}$$

where Z is the altitude of the considered site in kilometers [64].

4.1.10. Zabara model

Zabara suggested monthly values to the coefficients a and b of the Angstrom–Prescott–Page model with monthly relative sunshine duration (s/s_0) as a third order function and expressed a and b as follows [74]:

$$a = 0.395 - 1.247\left(\frac{S}{S_0}\right) + 2.680\left(\frac{S}{S_0}\right)^2 - 1.647\left(\frac{S}{S_0}\right)^3 \tag{40}$$

$$b = 0.395 + 1.384\left(\frac{S}{S_0}\right) - 3.249\left(\frac{S}{S_0}\right)^2 + 2.055\left(\frac{S}{S_0}\right)^3 \tag{41}$$

4.1.11. Kilic and Ozturk model

Kilic and Ozturk provided empirical values of the a and b parameters of the Angstrom–Prescott–Page model for Turkey as follows [75]:

$$a = 0.103 + 0.000017Z + 0.198\cos(\varphi - \delta) \tag{42}$$

$$b = 0.533 + 0.165\cos(\varphi - \delta) \quad (43)$$

4.1.12. Gariepy's model

Gariepy has expressed empirically the coefficients a and b of the Angstrom–Prescott–Page model in terms with mean air temperature T and the amount of precipitation (P) [76]:

$$a = 0.3791 - 0.0041T - 0.0176P \quad (44)$$

$$b = 0.4810 + 0.0043T + 0.0097P \quad (45)$$

4.1.13. Almorox and Hontoria model

Almorox and Hontoria suggested an exponential model as follows [77]:

$$\frac{H}{H_0} = a + b\exp\left(\frac{S}{S_0}\right) \quad (46)$$

4.1.14. Ampratwum and Dorvlo model

Ampratwum and Dorvlo proposed the following model [78]:

$$\frac{H}{H_0} = a + b\log\left(\frac{S}{S_0}\right) \quad (47)$$

4.1.15. Ogelman et al. model

Ogelman et al. have correlated (H/H_0) with (S/S_0) in the form of a second order polynomial equation [79]:

$$(a)\quad \frac{H}{H_0} = a + b\left(\frac{S}{S_0}\right) + c\left(\frac{S}{S_0}\right)^2 \quad (48)$$

$$(b)\quad \frac{H}{H_0} = 0.195 + 0.676\left(\frac{S}{S_0}\right) - 0.142\left(\frac{S}{S_0}\right)^2 \quad (49)$$

where a, b and c are experimental coefficients.

4.1.16. Samuel model

The ratio of global to extraterrestrial radiation was expressed by a function of the ratio of sunshine duration as follows [80]:

$$(a)\quad \frac{H}{H_0} = a + b\left(\frac{S}{S_0}\right) + c\left(\frac{S}{S_0}\right)^2 + d\left(\frac{S}{S_0}\right)^3 \quad (50)$$

$$(b)\quad \frac{H}{H_0} = 0.14 + 2.52\left(\frac{S}{S_0}\right) - 3.71\left(\frac{S}{S_0}\right)^2 + 2.24\left(\frac{S}{S_0}\right)^3 \quad (51)$$

where a, b and c are empirical coefficients.

4.1.17. Allen model

Allen developed a self adjusting model which is a function of the daily extraterrestrial radiation, mean monthly maximum and minimum temperature [81]:

$$\frac{H}{H_0} = a(T_{\max} - T_{\min})^{0.5} + b \quad (52)$$

4.2. Monthly-averaged hourly radiation

The second group of methods deals with the estimation of the monthly-averaged hourly solar-radiation. One of the most used models among this category is the ASHRAE clear-sky model [82]. In this model, the direct normal irradiation is estimated by means of a simple equation including two constants A and B while the diffuse radiation is given as a fraction C of the direct normal component.

The hourly global solar radiation on horizontal plane Q_h is composed by a beam (direct) radiation Q_{bh} and a diffuse sky radiation Q_{dh}.

The beam radiation Q_{bh} is given by the following formula [82]:

$$Q_{bh} = Q_n \times \cos\theta_z \quad (53)$$

where Q_n and θ_z are the normal direct radiation and θ_z is the zenith angle respectively.

The diffuse sky radiation Q_{dh} can be expressed as yields:

$$Q_{dh} = Q_n \times C \quad (54)$$

where C is the diffuse-sky factor.

Therefore, the global radiation on horizontal surfaces is:

$$Q_{dh} = Q_n \times \cos\theta_z + Q_n \times C \quad (55)$$

We note that direct normal radiation Q_n is calculated as the following:

$$Q_n = A \times \exp(-B/\sin\alpha_S) \quad (56)$$

where A is the apparent solar-radiation constant, B is the atmospheric extinction coefficient, and α_S is the solar altitude angle above the horizontal (the complement of the zenith angle).

ASHRAE [82] gave 12 sets of these three constants for each month of the year. The different sets of these constants are related to the monthly variation of the amount of precipitate water during the year. Hence, the twelve sets of ASHRAE's coefficients reflect the annual variation of the absolute atmospheric humidity [83]. In fact, the constant A is related to the solar constant while the variations of the constants B and C indicate a variation in turbidity as well. In order to account for regional variations of humidity and turbidity, ASHRAE published maps for a parameter called "clearness index", for both summer and winter, for different regions in the USA. This factor changes the values of amount radiation estimated by the model. Unfortunately, the unavailability of these factors for other regions of the world prohibited the use of this model for these regions. For this reason, several research works are focused to develop adjustment factors to the ASHRAE clear-sky model for many countries over the entire world. For instance, Powell [84] examined The ASHRAE model basing on data collected at 31 NOAA (National Oceanographic and Atmospheric Administration, USA) monitoring stations. The results established the universal validity of the model in predicting the solar radiation under cloudless conditions. Powell modified the basic ASHRAE model using altitude corrected optical air mass instead of seasonal clearness indexes. The author concluded that his modifications made the model generally more truthful. Machler and Iqbal [85] used the above modifications made by Powell to the ASHRAE model and adjusted the constants A, B, and C. Also, they introduced a correction humidity factor to account the variability of the water-vapor absorption.

Galanis and Chatigny [86] criticized some formulations of the ASHRAE model. The authors proposed to include the clearness index in the expressions of the direct and more importantly in the diffuse radiation under cloudless conditions. Moreover, they suggested to re-write expressions for cloudy-sky conditions in order reduce to the cloudless formulation for zero cloud cover.

Maxwell [87] developed the METSTAT solar radiation model (called METSTAT model) basing on data collected by 29 US National Weather Service sites. The model estimated the hourly values of direct normal, diffuse, and global solar radiation. The model requires some inputs such as the aerosol optical depth, the surface albedo, the snow depth, the atmospheric pressure, the precipitable water vapor and so forth. Even though, this model seems to be comprehensive, its application is restricted to regions where the above input data are available.

Rigollier et al. [88] developed another clear-sky model in the framework of the new digital European Solar Radiation Atlas (ESRA). The factors in the model have been empirically adjusted

by fitting techniques basing on hourly measurements over several years for a number of European regions.

Gueymard [89] suggested two models to calculate the monthly-average hourly global irradiation distribution from its monthly-averaged daily counterpart. He claimed that a quadratic expression in the sine of the solar elevation angle fitted accurately the data at all considered locations. The author included other parameters in his proposed models such as the mean monthly clearness index, the average day-length, and daily average solar elevation. He used a large data set from 135 stations covering diverse geographic locations and he confirmed the performance of those models presenting better relative precision compared to other previous models.

Yang and Koike [90] suggested a numerical model to predict the hourly-mean global solar-radiation taking account the upper-air humidity. The authors defined a sky-clearness indicator as a function of the relative humidity profiles in the upper atmosphere; then they used this indicator to relate global solar radiation under cloudy skies to that under clear skies.

4.3. Conventional way of estimating hourly solar radiation

The following calculations of the global solar flux on a horizontal plane are based on a conventional model [91] which assumes that the amount of direct radiation, I, intercepted by a perpendicular surface to the sun rays which are expressed as follows:

$$I = G_{sc} \times \exp\left[-\frac{TL}{0.9+9.4\sin\alpha_s}\right] \tag{57}$$

where G_{sc}, TL and α_S are the solar constant, the Linke's trouble factor and the solar altitude respectively. The Linke's trouble factor TL is expressed as the following:

$$TL = 2.4+14.6\beta+0.4(1+2\beta)\ln\left(p_p\right) \tag{58}$$

where β and p_p are the atmospheric trouble and the partial pressure respectively.

The value of β depends on atmospheric conditions of the site in question; β=0.05 in rural zone, β=0.1 in urban zone, β=0.2 in industrial park or polluted.

The partial pressure of steam p_p (expressed in mm Hg) can be calculated by the following equation:

$$p_p = \frac{760}{101325}(P_{at}-P_{dr}) \tag{59}$$

where P_{at} and P_{dr} are the atmospheric pressure (in Pascal) and the pressure of the dry air (equal to 101222.105 Pa) respectively.

The solar altitude α_S, which is the angle between the horizontal and the line to the sun, can be given using the following relation:

$$\sin\alpha_s = \sin\varphi\sin\delta+\cos\varphi\cos\delta\cos w \tag{60}$$

where φ is the latitude of the site which is the angular location north or south of the equator, north positive $-90^\circ \leq \varphi \leq +90^\circ$.

The hour angle ω is the solar angular displacement east or west of the local meridian due to the rotation of the earth (15° per hour). The hour angle is negative in the morning and positive afternoon. Therefore, the hour angle can be written as follows:

$$\omega = (t_S-12)15^\circ \tag{61}$$

where t_S is the solar time. It is known that converting civil time, t_C, to solar time t_S, requires that two corrections should be applied; the first one is the correction for the difference in longitude λ between the observer's meridian and the meridian on which the civil time is based, the second correction is from the equation of time ET. Solar time and equation of time are expressed by Eqs. (62) and (63):

$$t_S = t_C+\frac{\lambda}{15}-Z_C+ET \tag{62}$$

where Z_C is the time zone east of GMT.

$$ET = -(0.0002-0.47497\cos(B)+3.2265\cos(2B) +0.0903\cos(3B)+7.3509\sin(B)+9.392\sin(2B) +3.3361\sin(3B)) \tag{63}$$

where B is the mean anomaly of the earth, called also the fractional year, which is a parameter relating position and time for the earth moving in a Kepler orbit. It is what the true anomaly would be if the earth moved with constant speed along a perfectly circular orbit around the sun in the same time.

According to this model, the beam solar radiation component G_b received by a horizontal surface is given by the following equation:

$$G_b = G_{sc} \times \exp\left[-\frac{TL}{0.9+9.4\sin\alpha_s}\right] \times \sin\alpha_s = I \times \sin\alpha_s \tag{64}$$

The diffuse solar radiation component G_b is calculated by the following formula:

$$G_d = 54.8\sqrt{\sin\alpha_s}[TL-0.5-\sin\alpha_s] \tag{65}$$

The global solar radiation on horizontal surface, G_T, is the sum of the diffuse radiation, G_d and the beam radiation. Therefore, the incident global radiation on horizontal surface is given by the following expression:

$$G_T = G_d+G_b = G_{sc} \times \exp\left[-\frac{TL}{0.9+9.4\sin\alpha_s}\right] +54.8\sqrt{\sin\alpha_s}[TL-0.5-\sin\alpha_s] \tag{66}$$

5. Experimental results

In this section of study we are interested to the treatment of data registered by the NRG weather station installed on the site. This meteorological station is equipped by very precise and reliable instruments allowing the measure of the global stream of solar energy on a horizontal plane by way of a pyranometer (class A), the statement of ambient temperature and the sun covering rate. The programmed time step of the measurements is

Table 1
Ambient temperature characteristics.

	Ambient Temperature (°C)		
	2008	**2009**	**2010**
January	11.88	11.81	12.71
February	11.96	11	12.81
March	13.81	13.4	8.33
Apri	16.95	15.34	17.16
May	19.89	19.72	19.23
June	23.29	23.29	22.28
July	26.62	26.39	26.25
August	26.66	27.84	26.28
September	24.32	24.14	23.76
October	21.38	19.96	20.72
November	16.20	17.37	16.60
December	11.87	17.19	13
	Minimum Ambient Temperature (°C)		
	1.517	1.529	1.519
	Maximum Ambient Temperature (°C)		
	40.37	41.33	41.17
	Average Ambient Temperature (°C)		
	18.70	18.94	21.97

10 min. We note that solar radiation and sunshine duration has been abundantly measured in the country. A few attempts to develop knowledge about the variation of global solar radiation in Tunisia have been found in the literature. Thus, the aim of this paper is to assess the potential of solar energy resource in the gulf of Tunis. The statically measurements allow us to evaluate the average sun duration and the average solar flux during the years 2008, 2009 and 2010. Also, the accuracy degree of the conventional model to the experimental data is investigated.

5.1. Ambient temperature and global solar flux

Table 1 recapitulates the characteristics of the ambient temperature during the last three years. These measurements (157,860 samples) are provided by the NRG weather station with a step of 10 min. The variation of the ambient temperature during the three years is shown in Fig. 4. It is observed in the first six months of each year that the ambient temperature has the trend to increase from the lowest temperatures in December surrounding 10 °C to the highest temperatures in the summer months surrounding 30 °C. However, in the second half of the year the ambient temperature decreases till the end of the year. It is worth noting that the ambient temperature has nearly the same trend of variation during the three years. One can observe also that during the three years the average ambient temperature increases from 18.70 °C in 2008 to 21.97 °C in 2010.

Table 2 illustrates the variation of the global solar radiation on a horizontal surface during the last three years. It is observed that the peak of average monthly radiation in the gulf of Tunis is registered in July with the value of 230 kW/m^2 while the least is December with the value of 63 kW/m^2. The total annual global solar-radiation received in the Gulf of Tunis on a horizontal surface is 1681, 1763 and 1704 kWh/m^2 during 2008, 2009 and 2010 respectively. It is noticeable that the sunshine durations are important with the values of 3337, 3505 and 3415 h during 2008, 2009 and 2010 respectively. One can observe also that that more than 38% of this total global solar flux is contributed in the summer months.

Fig. 5 shows the monthly variation of global solar flux as hourly values, one can deduce obviously that the global solar flux has the same trend of variation as the ambient temperature presented in Fig. 4. Also, we find the highest global solar radiation values occurs in the summer months (June, July and August), while the lowest values lie in the winter months (December, January and February) and the global solar radiation values are seen to be equal through the autumn and spring months. This is because in the northern hemisphere, the sun's elevation angle during winter (November, December, and January) is lower than during the other seasons [92]. It is explained by the fact that the mean distance between the Earth and the Sun in winter is less than that in spring (or autumn) by about 3% due to the eccentricity of the Earth's orbit, resulting in a stronger flux of radiation. One can deduce that the variation of the global solar flux has the inverse trend of the zenith angle variation of the sun during the year. In the gulf of Tunis and in other mid-latitude countries north of the equator, the sun's daily trip is an arc across the southern sky. The sun's greatest height above the horizon occurs at noon, and how high the sun then gets depends on the season of the year, it is the highest in mid-summer (June), which correspond to the lowest zenith angle value, the lowest in mid-winter (December) that correspond to the highest zenith angle value.

Table 2
Global solar radiation characteristics.

Period	2008	2009	2010	Average/month
January	81	62	69	71
February	98	84	95	92
March	133	145	127	135
April	179	155	157	163
May	187	230	187	201
June	220	244	217	227
July	223	238	228	230
August	189	203	202	198
September	122	142	138	134
October	107	109	110	109
November	81	86	76	81
December	61	65	64	63
Average	**140,109**	**146,992**	**139,233**	**142,111**

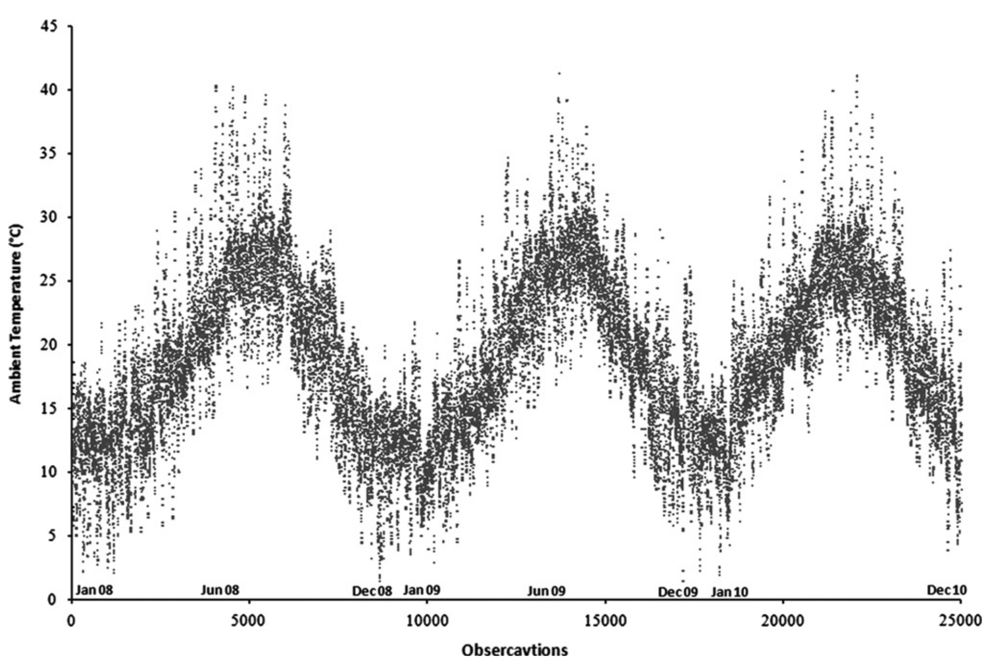


Fig. 4. Ambient temperature variation.

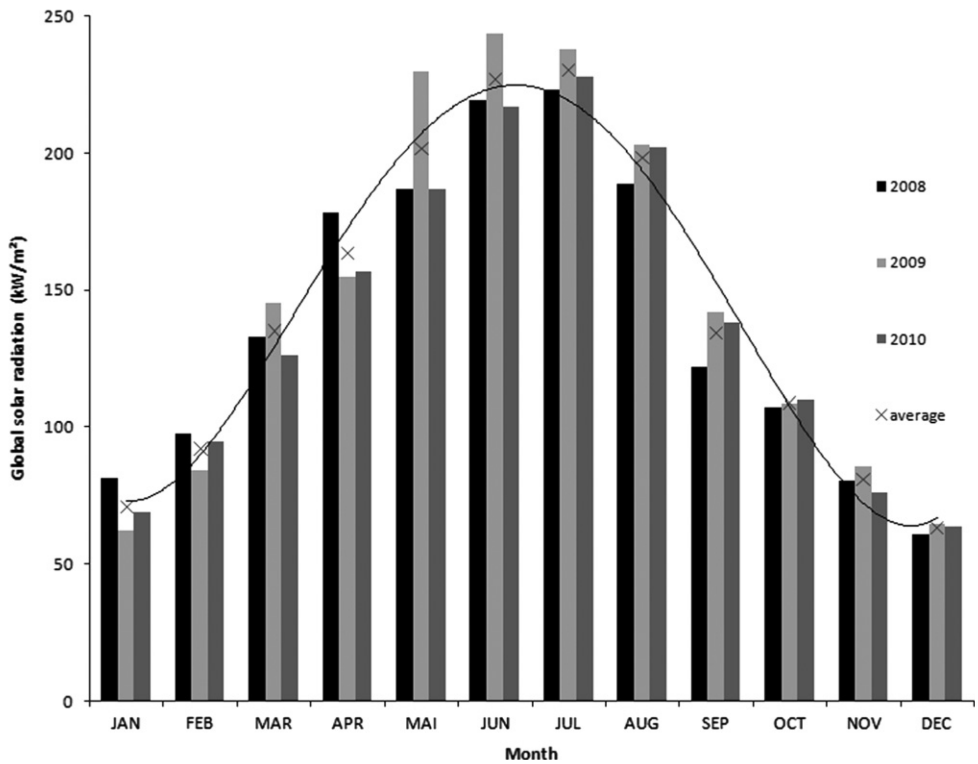


Fig. 5. Monthly variation of the global solar radiation.

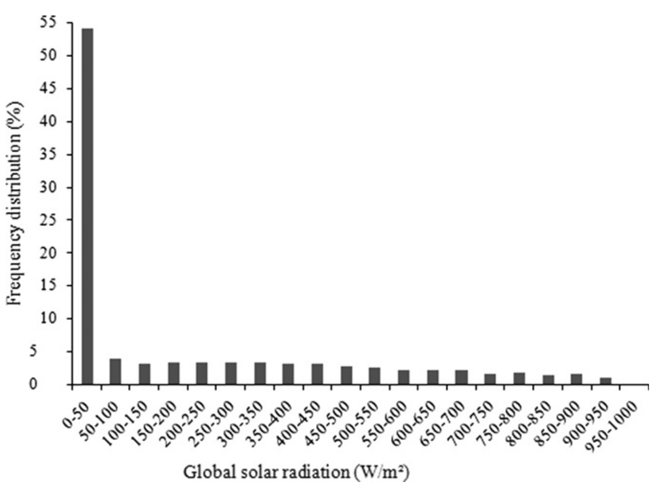


Fig. 6. Yearly frequency distribution of global solar radiation.

Hence, this trend of variation can be related to how high in the sky the sun appears.

5.2. *Yearly and seasonal probability distribution of global solar radiation*

Fig. 6 shows the yearly probability distribution or the fraction of time, based on the averaged hourly measurement of the global solar radiation of the three last years where they are within the interval given by the width of the columns (here 50 W/m^2 is selected). A global solar radiation frequency histogram is obtained by dividing the number of observations in each bin by the total number of observations in the data set. As shown from Fig. 6, the highest peak frequencies corresponds to the range of global solar radiation between 0 and 50 W/m^2 with a value equal to 54.15%. Concerning the other ranges of solar radiation, the highest frequency is related to the bin 250–300 W/m^2 with a value of 3.39% while the lowest one corresponds to the range of solar radiation within 950–1000 W/m^2 with a value equal to 0.11%. We can observe that all the other range of solar radiation have near values of frequency distribution.

Fig. 7(a)–(d) show the seasonal frequency distributions of global solar radiation based on the data of the three last years (2008, 2009 and 2010). Concerning the winter season, according to Fig. 7(a) and ignoring the solar radiation within 0 and 50 W/m^2 which corresponds almost to the night periods, it is observed that the prevalent range of global solar radiation is related to the range of 200–250 W/m^2 with a probability of 5.23%. It is worth noting also that during this season the radiations greater than 550 W/m^2 have a very low occurrence probability due to the cloudy periods of this season. Fig. 7(b) shows the frequency distribution of the global solar radiation in the summer season. It is observed that the highest frequency is related to the range of solar radiation 750–800 W/m^2 with a value of 4.48% while the lowest frequency corresponds to the radiation values between 950 and 1000 W/m^2. It is noticeable that all ranges of global solar radiation have significant values of occurrence probability due to the significant sunny months of this season. As shown in Fig. 7(c), the frequency of the global solar radiation during the autumnal months follow a similar distribution pattern but the peak of frequency corresponds to the solar radiation which falls in the range of 50–100 W/m^2 with a value equal to 4.21% because this radiation can be registered both during the sunrise and the sunset while the important radiations such those within 950 and 1000 W/m^2 can be recorded only during the hours surrounding the noon that is why their occurrence probability are very low compared relatively to the lowest radiations. During this season, the registered global solar radiation did not exceed the value of 800 W/m^2 and it is attributed mainly to the cloudy sky conditions of the autumnal months and the elevation of the sun. Fig. 7(d) shows that during the spring season the global solar radiation spread reaching the 1000 W/m^2 in comparison relatively to the autumn and winter

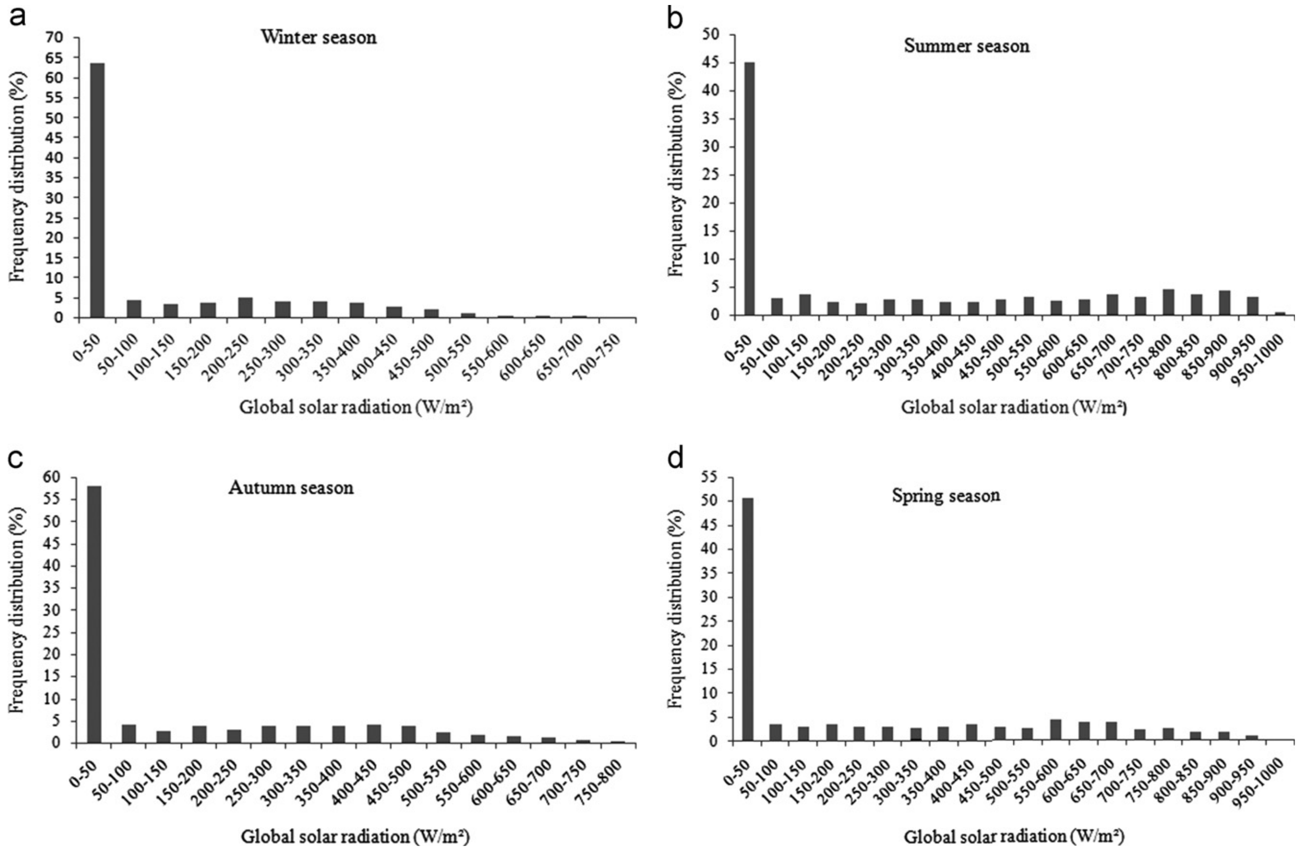


Fig. 7. Frequency distribution of global solar radiation during winter season (a), summer season (b), autumn season (c) and spring season (d).

seasons. On can observe also that with ignoring the solar of radiation that falls in the range of 0–50 W/m^2, the prevalent solar radiation corresponds to whose falls in the range of 550–600 W/m^2 with a probability of 4.08% while the infrequent solar radiations are related to whose falls within 900 and 1000 W/m^2 with a frequency of 0.84%. The obtained outcomes give good information about the solar radiation availability in the studied site and confirm again that the gulf of Tunis presents an important solar potential.

5.3. *Comparison of results and test of model*

Fig. 8(a)–(d) show the comparison between the measured global solar flux and the predicted one using a conventional model during four specific days. We note that these specific days correspond to the summer and winter solstice days and the vernal and autumnal equinox days. It is found that the conventional model consistently over-predicts the measurements at all times. This is expected since the model does not account for local weather conditions such as the presence of cloud and dust. Moreover, one can observe that there are visible discrepancies between the measurements for the three years. The performance of the conventional model was evaluated in terms of the relative percentage error (MAPE).Table 3 summarizes the MAPE of each year (2008, 2009 and 2010) as well as the global error for the whole samples during the four above-mentioned days. It is found that the highest global MAPE is occurred in the autumnal equinox, winter solstice and vernal equinox days with values of 14.26%, 14% and 10.34% respectively. This is generally attributed to the local cloud formations in these wintry, autumnally and vernally days which obviously vary from year-to-year. In contrast, the results presented for the summer solstice day in Fig. 8(b) show that both the measurements and the conventional model predictions differ only slightly. In fact, there is a practically close agreement between the results of the conventional model and the mean values of the measurements with a slight over-prediction of the global solar radiation received by a horizontal plane by the conventional model with a global MAPE equal to 4.10%. Results for the other days of the years, which are not presented here follow a similar trend and agree with the above conclusion, i.e. some discrepancies occur among the measurements for different years and with the predictions for the cloudy periods, namely, October–May. These differences decrease obviously for the months of June–September (summer months) for which the sky is relatively clearer.

The promising similarities between the measured and predicted solar-flux variations during the clear-sky dates suggest that global solar radiations have to estimated basing on this conventional model but it is will be more interesting to focused on refining a specific theoretical model concerning the gulf of Tunis.

6. Conclusion

The determination of global solar radiation as well as its real distribution at any site is vital important for many scientific, engineering and environmental applications. In this context, this paper is subscribed by the assessment of the solar energy potential in the gulf of Tunis, Tunisia. In fact, the ambient temperature, the global solar flux, the sun duration, the yearly and the seasonal frequency distribution of the global solar radiation were presented. The results proved that the site of Borj-cedria in the gulf of Tunis has been endowed by a promising solar energy potential. A conventional model of the global solar flux estimation was validated by the measurements data in

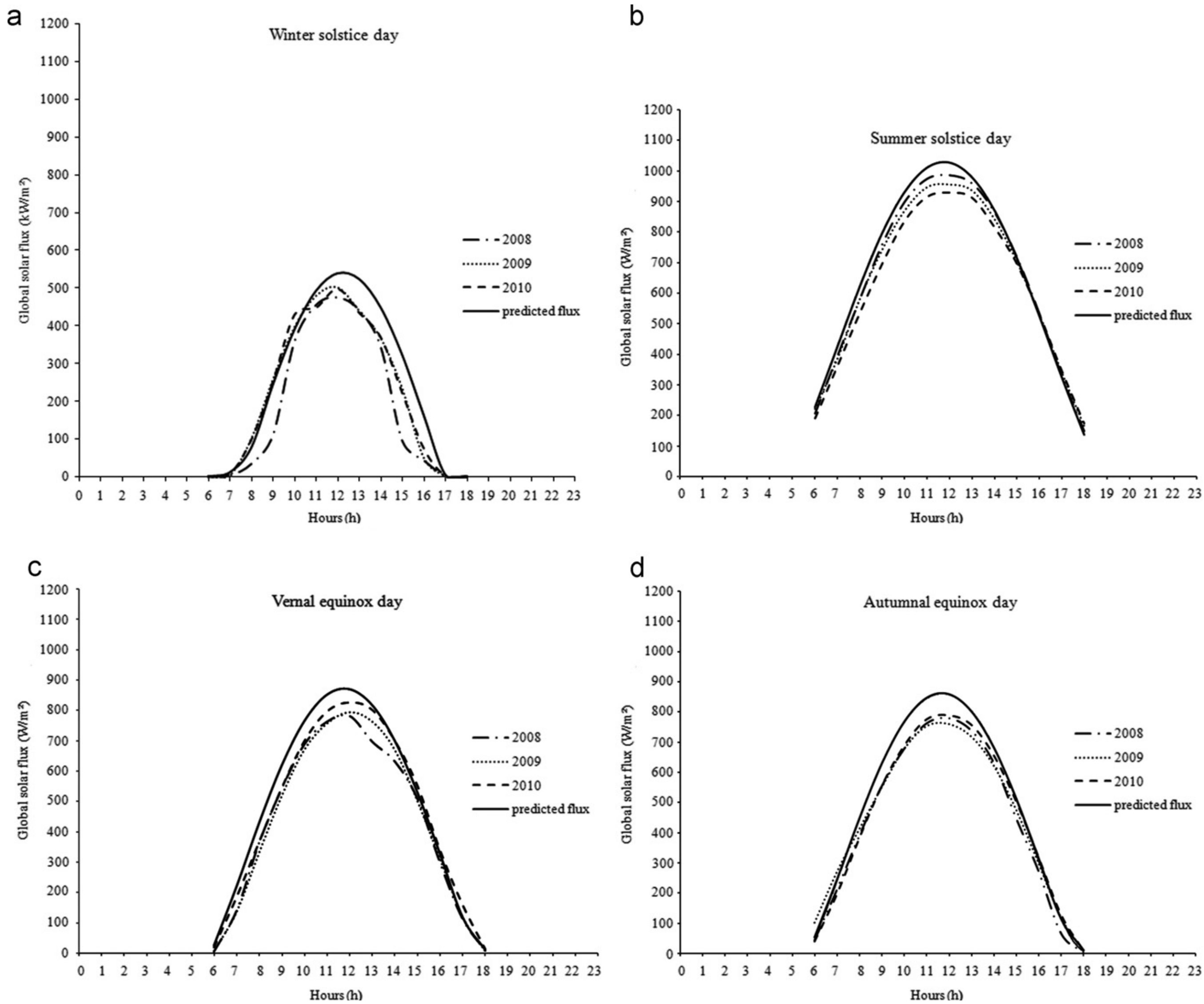


Fig. 8. Comparison between the predicted and the measured Global solar radiation during the winter solstice (a), summer solstice (b), vernal equinox (c) and autumnal equinox (d) days.

Table 3
Relative error percentage between the daily predicted and the measured global solar radiation.

	REP 2008 (%)	REP 2009 (%)	REP 10 (%)	Global REP (%)
Winter solstice day	15.89	18.14	8.56	14.2
Summer solstice day	3.49	2.66	6.16	4.1
Autumnal equinox day	14.49	12.79	15.49	14.26
Vernal equinox day	11.36	6.18	13.75	10.34

critical days of the last three years. A daily comparison basing on the mean absolute percentage error showed that this model predicted with good accuracy the real data under the clear sky conditions with an error of 4.10% while its performance decreases in the cloudy conditions with an error reaching the value of 14.26%. Hence, it is recommended to develop an appropriate site model in order to predict satisfactory the global solar flux in the gulf of Tunis. Finally, this aim is very important because if there are missing data for some months due to faulty operation of the measuring device, the developed model would be very useful used to predict the missing monthly global solar radiation at any date in the gulf of Tunis.

References

[1] Kalogirou SA. Solar thermal collectors and applications. Progress in Energy and Combustion. Science (New York, NY) 2004;30:231–95.

[2] Anderson B. Solar energy: fundamentals in building design. New York: McGraw-Hill; 1977.

[3] Meinel AB, Meinel MP. Applied solar energy: an introduction. Reading, MA: Addison-Wesley; 1976.

[4] Malik MAS, Tiwari GN, Kumar A, Sodha MS. Solar distillation. New York: Pergamon Press; 1985.

[5] Lysen E. Photovoltaics: an outlook for the 21st century. Renewable Energy World 2003;6:43–53.

[6] Rensheng C, Shihua L, Ersi K, Jianping Y, Xibin J. Estimating daily global radiation using two types of revised models in China. Energy Conversion and Management 2006;47:865–78.

[7] Bakirci K. Estimation of global solar radiation on horizontal surface. Journal of Thermal Science and Technology 2007;2:7–11.

[8] Bakirci K. Models of solar radiation with hours of bright sunshine: a review. Renewable and Sustainable Energy Reviews 2009;13:2580–8.

[9] Tahran S, Sarı A. Model selection for global and diffuse radiation over the Central Black Sea (CBS) region of Turkey. Energy Conversion and Management 2005;46:605–13.

[10] Aras H, Balli O, Hepbasli A. Global solar radiation Potential. Part 1. Model development energy sources Part B 2006;1:303–315.
[11] Bakirci K. Correlations for estimation of solar radiation on horizontal surface. Journal of Energy Engineering 2008;134:130–4.
[12] R. Kang E, Ji X, Yang J, Wang J. An hourly solar radiation model under actual weather and terrain conditions: a case study in Heihe river basin. Energy 2007;32:1148–57.
[13] Pandey CK, Katiyar AK. A note on diffuse solar radiation on a tilted surface. Energy 2009;34:1764–9.
[14] Evseev EG, Kudish AI. The assessment of different models to predict the global solar radiation on a surface tilted to the south. Solar Energy 2009;83:377–88.
[15] Robaa SM. Evaluation of sunshine duration from cloud data in Egypt. Energy 2008;33:785–95.
[16] Tomislav MP, Ivana SR, Dragana DM, Lana SP. A review of concentrating solar power plants in the world and their potential use in Serbia. Renewable and Sustainable Energy Reviews 2012;16:3891–902.
[17] Hacer D, Harun A. Sunshine-based estimation of global solar radiation on horizontal surface at Lake Van region (Turkey). Energy Conversion and Management 2012;58:35–46.
[18] Behrang MA, Assareh E, Noghrehabadi AR, Ghanbarzadeh A. New sunshine-based models for predicting global solar radiation using PSO (particle swarm optimization) technique. Energy 2011;36:3036–49.
[19] Sabziparvar AA, Shetaee H. Estimation of global solar radiation in arid and semi-arid climates of east and west Iran. Energy 2007;32:649–55.
[20] Sabziparvar AA. A simple formula for estimating global solar radiation in central arid deserts of Iran. Renewable Energy 2008;33:1002–10.
[21] Cucumo M, De Rosa A, Ferraro V, Kaliakatsos D, Marinelli V. Experimental testing of models for the estimation of hourly solar radiation on vertical surfaces at Arcavacata di Rende. Solar Energy 2007;81:692–5.
[22] Jacovidesa CP, Assimakopoulosb VD, Tymviosa FS, Theophilouc K, Asimakopoulosa DN. Solar global UV (280e380 nm) radiation and its relationship with solar global radiation measured on the island of Cyprus. Energy 2006;31:2728–38.
[23] Muzathik AM, Ibrahim MZ, Samo KB, Wan Nik WB. Estimation of global solar Irradiation on horizontal and inclined surfaces based on the horizontal measurements. Energy 2011;36:812–8.
[24] Coskum C, Oktay Z, Dincer L. Estimation of monthly solar distribution for solar energy system analysis. Energy 2011;36:1319–23.
[25] Ryder CL, Toumi R. An urban solar flux island: measurements from London. Atmospheric Environment 2011;45:3414–23.
[26] Ramachandra TV, Jaina R, Krishnadasa G. Hotspots of solar potential in India. Renewable and Sustainable Energy Reviews 2011;15:3178–86.
[27] Sorapipatana C. An assessment of solar energy potential in, Kampuchea. Renewable and Sustainable Energy Reviews 2010;14:2174–8.
[28] Molero VN, Cejudo LJM, Domínguez MF, Rodríguez GEA, Carrillo Andrés. Numerical 3-D heat flux simulations on flat plate solar collectors. Solar Energy 2009;83:1086–92.
[29] Hocaoglu FO. Stochastic approach for daily solar radiation modeling. Solar Energy 2011;85:278–87.
[30] Ozgoren M, Bilgili M, Sahin B. Estimation of global solar radiation using ANN over Turkey. Expert Systems with Applications 2012;39:5043–51.
[31] Maghrabi AH. Parameterization of a simple model to estimate monthly global solar radiation based on meteorological variables, and evaluation of existing solar radiation models for Tabouk, Saudi Arabia. Energy Conversion and Management 2009;50:2754–60.
[32] Mao FL, Liu Hong-Bin, Peng TG, Wei W. Estimation of daily solar radiation from routinely observed meteorological data in Chongqing, China. Energy Conversion and Management 2010;51:2575–9.
[33] Moradi I. Quality control of global solar radiation using sunshine duration hours. Energy 2009;34:1–6.
[34] Cyril V, Marc M, Christophe P, Marie LN. Optimization of an artificial neural network dedicated to the multivariate forecasting of daily global radiation. Energy 2011;36:348–59.
[35] Iranna Korachagaon, Bapat VN. General formula for the estimation of global solar radiation on earth's surface around the globe. Renewable Energy 2012;41:394–400.
[36] Si-qing L, Qiu-zhen Z, Jing W, Xian-kang D. Modeling Research of the 27-day Forecast of 10.7° cm solar radio flux. Chinese Astronomy and Astrophysics 2010;34:305–15.
[37] Dahmouni AW, Ben Salah M, Askri F, Kerkeni C, Ben Nasrallah S. Wind energy in Tunis, Tunisia. Renewable and Sustainable Energy Review 2010;14:1303–11.
[38] Tarhan S, Sari A. Model selection for global and diffuse radiation over the Central Black Sea (CBS) region of Turkey. Energy Conversion and Management 2005;46:605–14.
[39] Ulgen K, Hepbasli A. Comparison of solar radiation correlations for Izmir, Turkey. International Journal of Energy Research 2002;26:413–30.
[40] Ulgen K, Hepbasli A. Prediction of solar radiation parameters through clearness index for Izmir, Turkey. Energy Source 2002;24:773–85.
[41] Ulgen K, Hepbasli A. Estimation of solar radiation parameters for Izmir, Turkey. International Journal of Energy Research 2002;26:807–23.
[42] Jin Z, Yezheng W, Gang Y. General formula for estimation of monthly average daily global solar radiation in China. Energy Conversion and Management 2005;46:257–68.
[44] Togrul IT, Togrul H, Evin D. Estimation of monthly global solar radiation from sunshine duration measurements in Elazig. Renewable Energy 2000;19:587–95.
[45] Ertekin C, Yaldiz O. Estimation of monthly average daily global radiation on horizontal surface for Antalya, Turkey. Renewable Energy 1999;17:95–102.
[46] Ertekin C, Yaldiz O. Comparison of some existing models for estimating global solar radiation for Antalya (Turkey). Energy Conversion and Management 2000;41:311–30.
[47] Tadros MTY. Uses of sunshine duration to estimate the global solar radiation over eight meteorological stations in Egypt. Renewable Energy 2000;21:231–46.
[48] Chen R, Ersi K, Yang J, Lu S, Zhao W. Validation of five global radiation models with measured daily data in China. Energy Conversion and Management 2004;45:1759–69.
[49] El-Metwally M. Sunshine and global solar radiation estimation at different sites in Egypt. Journal of Atmospheric and Terrestrial Physics 2005;67:1331–42.
[50] Togrul IT, Onat E. A comparison of estimated and measured values of solar radiation in Elazig, Turkey. Renewable Energy 2000;20:243–52.
[51] Togrul IT, Togrul H, Evin D. Estimation of global solar radiation under clear sky radiation in Turkey. Renewable Energy 2000;21:271–87.
[52] Halawa EEH. Sugiyatno. Estimation of global solar radiation in the Indonesian climatic region. Renewable Energy 2001;24:197–206.
[53] Souza JL, Nicacio RM, Moura MAL. Global solar radiation measurements in Maceio, Brazil. Renewable Energy 2005;30:1203–20.
[54] Almorox J, Benito M, Hontoria C. Estimation of monthly Angström–Prescott equation coefficients from measured daily data in Toledo, Spain. Renewable Energy 2005;30:931–6.
[55] Almorox J, Hontoria C, Benito M. Statistical validation of day length definitions for estimation of global solar radiation in Toledo, Spain. Energy Conversion and Management 2005;46:1465–71.
[56] Elagib N, Mansell MG. New approaches for estimating global solar radiation across Sudan. Energy Conversion and Management 2000;41:419–34.
[57] Rehman S, Halawani T. Global solar radiation estimation. Renewable Energy 1997;12:369–85.
[58] Togrul IT, Onat E. A study for estimating solar radiation in Elazig using geographical and meteorological data. Energy Conversion and Management 1999;40:1577–84.
[59] Togrul IT, Togrul H. Global solar radiation over Turkey: comparison of predicted and measured data. Renewable Energy 2002;25:55–67.
[60] Tiba C, Aguiar R, Fraidenraich N. Analysis of a new relationship between monthly global irradiation and sunshine hours from a database of Brazil. Renewable Energy 2005;30:957–66.
[61] Chegaar M, Chibani A. Global solar radiation estimation in Algeria. Energy Conversion and Management 2001;42:967–73.
[62] Suehrcke H. On the relationship between duration of sunshine and solar radiation on the Earth's surface: Angstromös equation revisited. Solar Energy 2000;68:417–25.
[63] Angstrom A. Solar and terrestrial radiation. Quarterly Journal of the Royal Meteorological Society 1924;50:121–5.
[64] Prescott JA. Evaporation from water surface in relation to solar radiation. Transactions of the Royal Society of Australia 1940;46:114–8.
[65] Duffie JA, Beckman WA. Solar engineering of thermal process. New York: Wiley; 1991.
[66] Menges HO, Ertekin C, Sonmete MH. Evaluation of global solar radiation models for Konya, Turkey. Energy Conversion and Management 2006;47:3149–73.
[67] Page JK. The estimation of monthly mean values of daily total short wave radiation on vertical and inclined surfaces from sunshine records for latitudes 40 °N–40 °S. In: Proceedings of UN conference on new sources of energy; 1961. p. 378–90.
[68] Bahel V, Srinivasan R, Bakhsh H. Solar radiation for Dhahran, Saudi Arabia. Energy 1986;11:985–9.
[69] Louche A, Notton G, Poggi P, Simonnot G. Correlations for direct normal and global horizontal irradiation on a French Mediterranean site. Solar Energy 1991;46:261–6.
[70] Benson RB, Paris MV, Sherry JE, Justus CG. Estimation of daily and monthly direct, diffuse and global solar radiation from sunshine duration measurements. Solar Energy 1984;32:523–35.
[71] Dogniaux R, Lemoine M. Classification of radiation sites in terms of different indices of atmospheric transparency.Solar energy research and development in the European community, series F, 2. Dordrecht, Holland: Reidel; 1983.
[72] Soler A. Monthly specific Rietveld's correlations. Solar and Wind Technology 1990;7:305–8.
[73] Gopinathan KK. A simple method for predicting global solar radiation on a horizontal surface. Solar and Wind Technology 1988;5:581–3.
[74] Zabara K. Estimation of the global solar radiation in Greece. Solar and Wind Technology 1986;7:267–72.
[75] Kilic A, Ozturk A. Solar energy. Istanbul: Kipas Yayincilik; 1983 [in Turkish].
[76] Gariepy J. Estimation of global solar radiation. International report. Service of meteorology. Government of Quebec, Canada; 1980.
[77] Almorox J, Hontoria C. Global solar radiation estimation using sunshine duration in Spain. Energy Conversion and Management 2004;45:1529–35.
[78] Ampratwum DB, Dorvlo ASS. Estimation of solar radiation from the number of sunshine hours. Applied Energy 1999;63:161–7.
[79] Ogelman H, Ecevit A, Tasdemiroglu E. A new method for estimating solar radiation from bright sunshine data. Solar Energy 1984;33:619–25.
[80] Samuel TDMA. Estimation of global radiation for Sri Lanka. Solar Energy 1991;47:333–7.

[81] Allen R. Self calibrating method for estimating solar radiation from air temperature. Journal of Hydrologic Engineering 1997;2:56–67.
[82] ASHRAE. Handbook of fundamentals 1979. American society of heating, refrigeration, and air-conditioning engineers. New York; 1979.
[83] Al-Sanea SA, Zedan MF, Al-Ajlan SA. Adjustment factors for the ASHRAE clear-sky model based on solar-radiation measurements in Riyadh. Applied Energy 2004;79:15–237.
[84] Powell GL. The ASHRAE clear-sky model – an evaluation. ASHRAE Journal 1982:32–4.
[85] Machler MA, Iqbal M. A modification of the ASHRAE clear-sky irradiation model. ASHRAE Transactions 1985;91:106–15.
[86] Galanis N, Chatigny R. A critical review of the ASHRAE solar-radiation model. ASHRAE Transactions 1986;92:410–9.
[87] Maxwell EL. METSTAT–The solar radiation model used in the production of the national solar radiation data base (NSRDB). Solar Energy 1998;62: 263–79.
[88] Rigollier C, Bauer O, Wald L. On the clear-sky model of the ESRA – European solar radiation atlas – with respect to the Heliosat method. Solar Energy 2000;68:33–48.
[89] Gueymard C. Prediction and performance assessment of mean hourly global radiation. Solar Energy 2000;68:285–303.
[90] Yang K, Koike T. Estimating surface solar-radiation from upper-air humidity. Solar Energy 2002;72:177–86.
[91] Ozdamar A, Ozbalta N, Akin A, Yildirim ED. An application of a combined wind and solar energy system in Izmir. Renewable and Sustainable Energy Reviews 2005;9:624–37.
[92] Maatallah T, El Alimi S, Ben Nassrallah S. Performance modeling and investigation of fixed, single and dual-axis tracking photovoltaic panel in Monastir city, Tunisia. Renewable and Sustainable Energy Reviews 2011;15: 4053–66.